PNAS RESEARCH ARTICLE | SYSTEMS BIOLOGY

Plasma metabolome and cytokine profile reveal glycylproline modulating antibody fading in convalescent COVID-19 patients

Zhu Yang[a,b,c,1], Di Wu[d,e,1], Shanxin Lu[a,b,1], Yang Qiu[d,e,1], Zhengyi Hua[a,b], Fancheng Tan[a,b], Cixiong Zhang[a], Lei Zhang[a], Ding-Yu Zhang[e,f], Xi Zhou[d,e,f,2], Zongwei Cai[c,2], You Shang[e,f,g,2], and Shu-Hai Lin[a,b,2]

Edited by Wafik El-Deiry, Brown University; received September 30, 2021; accepted April 29, 2022 by Editorial Board Member Diane E. Griffin

The COVID-19 pandemic has incurred tremendous costs worldwide and is still threatening public health in the "new normal." The association between neutralizing antibody levels and metabolic alterations in convalescent patients with COVID-19 is still poorly understood. In the present work, we conducted absolutely quantitative profiling to compare the plasma cytokines and metabolome of ordinary convalescent patients with antibodies (CA), convalescents with rapidly faded antibodies (CO), and healthy subjects. As a result, we identified that cytokines such as M-CSF and IL-12p40 and plasma metabolites such as glycylproline (gly-pro) and long-chain acylcarnitines could be associated with antibody fading in COVID-19 convalescent patients. Following feature selection, we built machine-learning–based classification models using 17 features (six cytokines and 11 metabolites). Overall accuracies of more than 90% were attained in at least six machine-learning models. Of note, the dipeptide gly-pro, a product of enzymatic peptide cleavage catalyzed by dipeptidyl peptidase 4 (DPP4), strongly accumulated in CO individuals compared with the CA group. Furthermore, severe acute respiratory syndrome coronavirus 2 (SARS-CoV-2) vaccination experiments in healthy mice demonstrated that supplementation of gly-pro down-regulates SARS-CoV-2–specific receptor-binding domain antibody levels and suppresses immune responses, whereas the DPP4 inhibitor sitagliptin can counteract the inhibitory effects of gly-pro upon SARS-CoV-2 vaccination. Our findings not only reveal the important role of gly-pro in the immune responses to SARS-CoV-2 infection but also indicate a possible mechanism underlying the beneficial outcomes of treatment with DPP4 inhibitors in convalescent COVID-19 patients, shedding light on therapeutic and vaccination strategies against COVID-19.

metabolomics | cytokine profiling | convalescent COVID-19 patients | glycylproline | SARS-CoV-2

Significance

Using absolute quantification of both cytokines and metabolites from the plasmas of convalescent COVID-19 patients, machine-learning approaches identified that a combination of cytokines and metabolites can clearly discriminate convalescent patients with rapidly faded antibodies (CO) from ordinary convalescents with antibodies (CA). We found glycylproline (gly-pro) accumulation in CO individuals compared with the CA group. Intriguingly, gly-pro contributes to the rapid fading of severe acute respiratory syndrome coronavirus 2 (SARS-CoV-2)–specific antibodies, whereas the inhibitor of its producing enzyme dipeptidyl peptidase 4, an antidiabetic drug, can counteract the gly-pro–down-regulated SARS-CoV-2-specific antibodies under physiological conditions. Therefore, our findings point to a novel mechanism for gly-pro–suppressed immune responses upon SARS-CoV-2 infection and provide therapeutic potentials for maintaining neutralizing antibody levels.

To date more than 400 million people have caught COVID-19 and the death toll is around 6 million around the world. COVID-19 is caused by a β-coronavirus named severe acute respiratory syndrome coronavirus 2 (SARS-CoV-2), due to its nearly 80% genomic similarity to SARS-CoV (1), the pathogen causing the severe acute respiratory syndrome (SARS) outbreak in 2002. The worldwide epidemic of the disease necessitated the immediate and global dedication of a massive amount of resources and intelligence. After over 2 y, although most of the COVID-19 patients have recovered from the disease and billions of citizens have been vaccinated, the pandemic is still raging across the world. Deeper insights into the response and recovery processes of this disease are of value for risk prediction and for the most important follow-up issues such as vaccination strategies and herd immunity.

The rapidly accumulated data of patients and convalescents with COVID-19 have been characterized by heterogeneity in susceptibility and severity. The COVID-19 patients ranged from asymptomatic infections to ones with multiorgan failure. The interindividual variability of the disease has been associated with age, biological sex, ethnicity, and the presence of preconditions (2). One of the important heterogeneities is the interindividual biological difference in the production of antibodies against invading viruses and vaccines. The convalescents with low levels of anti–SARS-CoV-2 antibodies have drawn clinical concern since early on (3, 4). A study of the patients in Wanzhou District, Chongqing City, China reported that approximately a sixth of the infected were seronegative in SARS-CoV-2–specific immunoglobulin G (IgG) in their acute phase; in 12.9% symptomatic and 40% asymptomatic IgG-positive individuals, the virus-specific IgG antibodies have faded 8 wk after they were discharged from the hospital (5). The race of vaccine development against SARS-CoV-2 started immediately after the unprecedented breakout of the pandemic and billions of people have been vaccinated worldwide. However, it has been observed since the early phase of vaccine development that vaccine recipients showed variability up to three orders of magnitude in antibody production (6–9).

This article is a PNAS Direct Submission. W.E.-D. is a guest editor invited by the Editorial Board.

[1]Z.Y., D.W., S.L., and Y.Q. contributed equally to this work.

[2]To whom correspondence may be addressed. Email: zhouxi@wh.iov.cn, zwcai@hkbu.edu.hk, you_shanghust@163.com, or shuhai@xmu.edu.cn.

This article contains supporting information online at http://www.pnas.org/lookup/suppl/doi:10.1073/pnas.2117089119/-/DCSupplemental.

Published August 9, 2022.

It has also been reported that a small proportion of participants have not successfully seroconverted postvaccination, and the virus-specific antibodies in some seropositive individuals faded in a few months even after two doses of SARS-CoV-2 vaccination (10). The levels of neutralizing antibodies are highly associated with immune protection from SARS-CoV-2 infection (11). How many individuals can produce enough antibodies is crucial for herd immunity against this infectious disease. An autopsy study revealed that the fatal COVID-19 patients lacked germinal centers in their lymph nodes, which might impair their production of antibodies against SARS-CoV-2 (12). However, the underlying etiology of these interindividual variations in SARS-CoV-2–induced immune responses, especially the fast fading of SARS-CoV-2–specific antibodies in some patients, is still unclear.

Similar to many other infectious respiratory diseases, SARS-CoV-2 causes changes in plasma molecules. The alterations of cytokines are essential in host immune responses to SARS-CoV-2 infection. The plasma cytokines of severe COVID-19 patients were significantly higher (13, 14). Rapid cytokine release could cause acute respiratory distress syndrome and respiratory failure, which is called the cytokine storm, considered the main cause of mortality in COVID-19 patients (14, 15). Consistently, lower levels of cytokines, as well as virus-specific antibodies, characterized the weak immune response of asymptomatic COVID-19 patients, who had a longer duration of viral spreading than symptomatic ones (5). Clinical reports have demonstrated that the sera of COVID-19 patients have elevated levels of proinflammatory cytokines such as interleukin-6 (IL-6), IL-1β, interferon γ (IFNγ), C-X-C motif chemokine ligand 10 (CXCL10), and monocyte chemoattractant protein-1 (MCP1), similar to the cases of SARS-CoV and Middle East respiratory syndrome coronavirus (MERS-CoV) infections (14). The changes in plasma metabolome have also been tightly associated with viral infections. With the accumulation of COVID-19 cases, more and more studies have profiled the metabolomic changes in the sera of COVID-19 patients and convalescents (16–19). These studies demonstrated dramatic alterations in the pathways of macrophage function, platelet degranulation, complement system, and energy metabolism. In addition, integrative analysis of cytokines and metabolites in COVID-19 patients found that the changes in amino acids and purine metabolism might be correlated with proinflammatory cytokines (18). However, little is known about the traits of cytokines and metabolites associated with the receptor-binding domain (RBD)-specific antibody levels in convalescent COVID-19 patients.

Herein, we conducted absolute quantification of cytokines and circulating metabolites to profile the molecular alterations associated with two subgroups of convalescent COVID-19 patients, including convalescent patients with antibodies (normal convalescent patients; CA group) and antibody-faded convalescent patients (CO group). Our findings uncovered some COVID-19–associated alterations of host cytokines and metabolites in two different types of convalescent patients. Among these changed molecules, our data showed that aberrant metabolisms of gly-pro (glycylproline) and its producing enzyme dipeptidyl peptidase 4 (DPP4), also known as CD26 or glycylproline dipeptidyl aminopeptidase (GPDA), may contribute to the fast fading of SARS-CoV-2 antibodies in the CO group of convalescent COVID-19 patients. Importantly, we demonstrate that changes in circulating gly-pro and the activities of DPP4 altered the production of antibodies against the RBD of SARS-CoV-2 in immunized mice. This result demonstrates a possible reason for the beneficial effects of DPP4 inhibitors on COVID-19 patients clinically (20–22). Therefore, our study reveals the physiological changes in metabolism in different types of convalescent COVID-19 patients, and the findings here could help mechanistically understand how the inhibition of DPP4 can benefit COVID-19 patients.

Results

Study Design and Sample Collection. To explore the molecular characteristics of convalescent COVID-19 patients of various responses, we enrolled a cohort of convalescent patients (both the CA and CO groups) and healthy volunteers (the H group) at Wuhan Jinyintan Hospital and harvested their plasma samples (Fig. 1*A*). Absolute quantification then profiled the concentrations of inflammatory factors and metabolites in plasma, from which we identified molecules critical for distinguishing the patients of various groups and developed machine-learning methods for predicting the antibody response based on these selected features (Fig. 1*A*). The serological tests for SARS-CoV-2 RBD-specific IgG of all patients were positive during hospitalization. We defined them as CA and CO groups according to the antibody levels after their discharges from the hospital. The CO group are the convalescent patients who were seronegative in SARS-CoV-2–specific IgG within 40 to 70 d after the symptomatic onset, while the subjects positive in antibodies belonged to the CA group. In total, the present study has recruited 17 CA and 30 CO convalescents as well as 35 healthy volunteers (Fig. 1*B* and *SI Appendix*, Table S1). The male-to-female ratios of all groups were ∼55:45. The median age of the H, CA, and CO groups are 44 y (from 23 to 65 y), 61 y (from 31 to 73 y), and 45 y (from 26 to 67 y), respectively (Fig. 1*C*). The persistent days positive in COVID-19 RNA test data of the two patient groups were both 24 d, with the first and third quartiles of 22 and 27 for CA groups and 21 and 28 for CO patients, respectively (Fig. 1*D*). The Pearson's correlation coefficients of each pair of individuals across inflammatory cytokines demonstrated that according to our definition the individuals classified in the same groups shared highly similar characteristics in their immune system (Fig. 1*E*). Plasma cytokines of 78%, 70%, and 70% of intragroup pairs from the H, CA, and CO groups, respectively, show a positive correlation. Both convalescent patient groups had a relatively higher level of similarity, with 52% of intergroup pairs between the CA and CO subjects showing a positive correlation. In contrast, positive correlations observed from these "one-to-one" comparisons were only 36% between the H and CA groups and 24% between the H and CO groups. On the other hand, plasma metabolome showed higher diversity and no strongly correlated pattern was observed intra- or intergroup (Fig. 1*E*), suggesting that as all healthy subjects the fluctuation in their serum metabolites mainly came from the individual differences (23).

Cytokine Profiling of Convalescent COVID-19 Patients. To determine the cytokine signature associated with antibody fading in the recovered COVID-19 patients, we measured the plasma concentrations of 38 inflammatory factors in all 35 healthy controls and 47 COVID-19 convalescent patients (17 CA and 30 CO) (Fig. 2*A* and *SI Appendix*, Table S2). The CA and CO groups had both common and differential alterations in these measured factors as compared with the healthy control. Noting the disparate age distribution across groups (Fig. 1*C*), we employed analysis of covariance (ANCOVA) to compare each measured inflammatory cytokine across the three groups considering the ages of the individuals as one of the two covariates (another covariate is sex). In total, 26 inflammatory cytokines differed significantly between at least two of the three groups (*SI Appendix*, Fig. S1), and seven cytokines including IL-12p40, IL-1 receptor antagonist (IL-1RA),

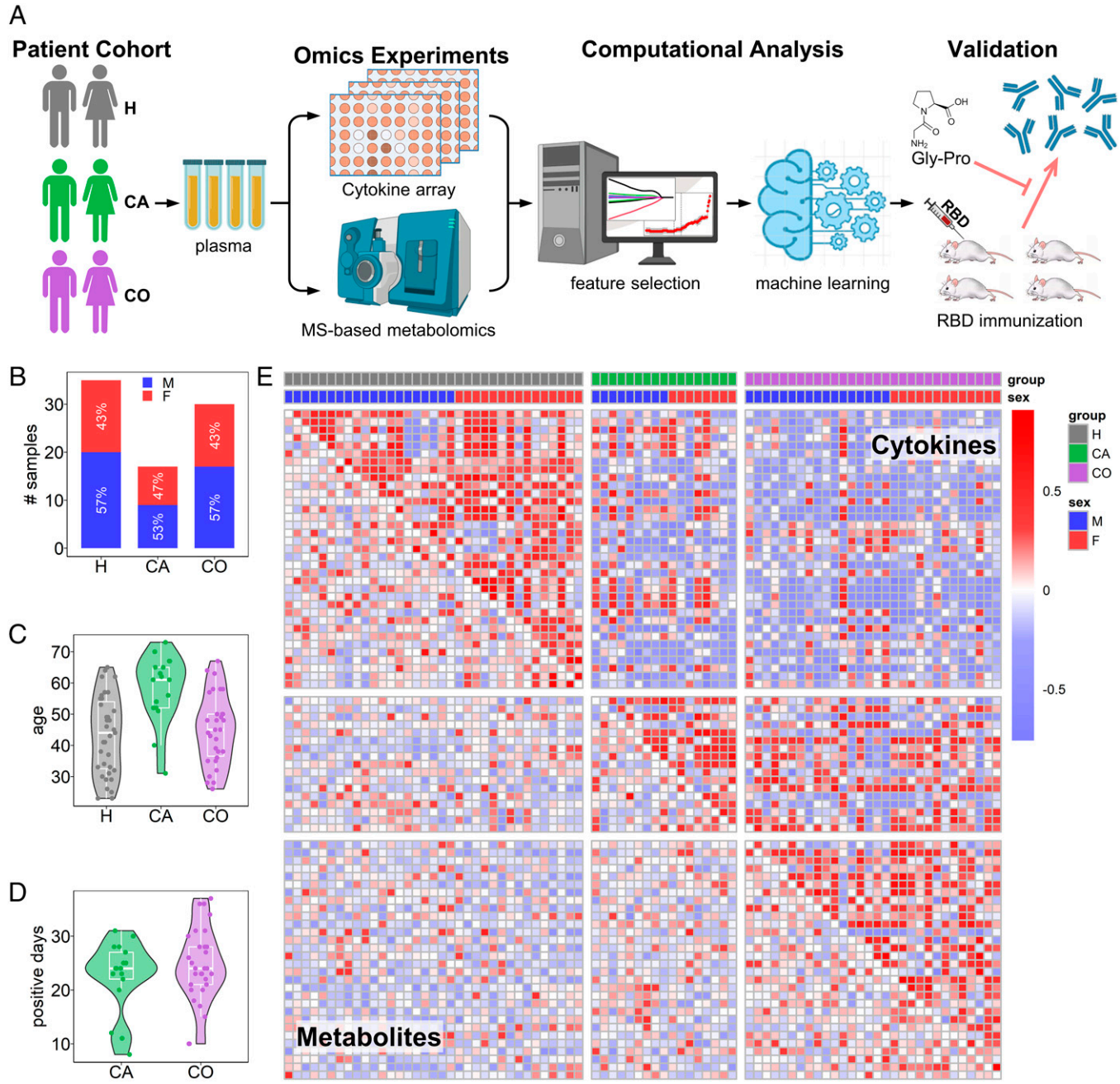

Fig. 1. The profile of the study. (*A*) The schematic diagram of the overall workflow. The plasma of two groups of cured COVID-19 patients and healthy control (H) were collected. The two groups are convalescent patients with antibody (CA) and antibody-faded convalescent patients (CO). Both cytokines and metabolites were absolutely quantified and the critical features (either cytokines or metabolites) were selected using machine learning and validated in mice. (*B*–*D*) The number of individuals (*B*), age (*C*), and COVID-19–positive days (*D*) of each group. (*E*) The Pearson's correlation coefficients of every two individuals across all inflammatory factors (upper triangle) and metabolites (lower triangle) measured. Self-correlations are identified in white.

macrophage colony-stimulating factor (M-CSF), B lymphocyte chemoattractant (BLC), IL-6 receptor (IL-6R), tumor necrosis factor receptor II (TNF-RII), and intercellular adhesion molecule 1 (ICAM-1) showed distinct profiles between the CA and CO groups (Table 1). As expected, the comparisons between convalescent patients (CA or CO) and healthy subjects showed more differentially expressed cytokines (16 in the comparison between the H and CA groups and 24 in the comparison between the H and CO groups) (*SI Appendix*, Fig. S1).

Although most of the altered cytokines showed the same trends in both convalescent groups, the CA and CO individuals had distinct immune responses to SARS-CoV-2 infection. TNFα (Fig. 2*B*), one of the most prominent cytokines predicting COVID-19 severity and mortality (24), IFNγ (Fig. 2*C*), the cytokine inhibiting viral replication, TNFβ, granulocyte-macrophage colony-stimulating factor (GM-CSF), and tissue inhibitor of metalloproteinases 1 (TIMP1) and TIMP2 (*SI Appendix*, Fig. S1*A*) showed higher levels in the convalescents compared with the healthy group, suggesting that convalescent patients are still abnormal in their immune system. Not quite alike, the cytokines IL-12p40, IL-1RA, and BLC and the cytokine receptors IL-6R and TNF-RII also declined in both groups of convalescent individuals with even lower levels in the CO group (Fig. 2 *D* and *E* and *SI Appendix*, Fig. S1*B*). A similar alteration pattern had also been observed in the other 10 cytokines, although only their changes in the CO group were

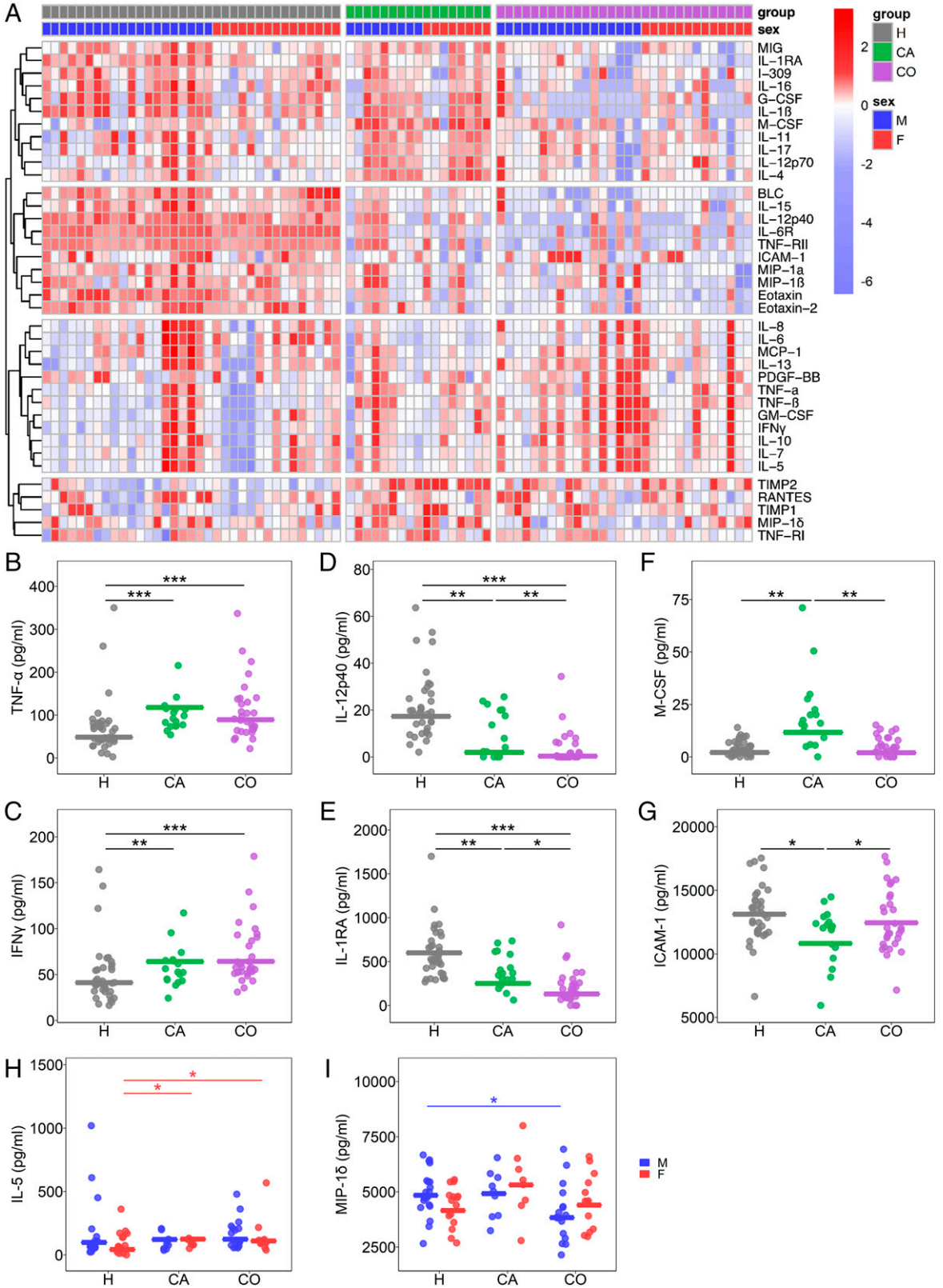

Fig. 2. The absolute quantification of inflammatory factors. (*A*) The Z-score of cytokines of all three groups. (*B*–*G*) The representatives of the cytokines that showed significant alterations among the three groups, including TNF-α (*B*), IFNγ (*C*), IL-12p40 (*D*), IL-1RA (*E*), M-CSF (*F*), and ICAM-1 (*G*). (*H* and *I*) The levels of IL-5 (*H*) and MIP-1δ (*I*) significantly changed only between different groups of the same sex. The significance was obtained by ANCOVA employing both age and sex (*B*–*G*) or only age (*H* and *I*) as covariates. *$q < 0.05$; **$q < 0.01$; ***$q < 0.005$.

significant (*SI Appendix*, Fig. S1*C*). Of great interest is only two cytokines with specific changes in the CA individuals. An enhanced level of M-CSF and decreased ICAM-1 were observed in the CA rather than the CO group (Fig. 2 *F* and *G* and *SI Appendix*, Fig. S1*D*). The CO individuals had mean levels of M-CSF (2.0 pg/mL) and ICAM-1 (13.1 ng/mL) very similar to those (2.1 pg/mL of M-CSF and 12.4 ng/mL of ICAM-1) in the healthy subjects (see Fig. 4 *F* and *G*), whereas M-CSF and

Table 1. The altered cytokines and metabolites from ANCOVA comparison and LASSO feature selection

	Changed between CA and CO		Selected by LASSO using MLRR	
	Molecule	CO/CA	Molecule	CO/CA
Cytokines	IL-12p40	0.16	IL-12p40	0.16
	M-CSF	0.17	M-CSF*	0.17
	BLC	0.29	IL-6R	0.36
	IL-6R	0.36	Eotaxin	0.76
	IL-1RA	0.52	TIMP2	0.94
	TNF-RII	0.60	TIMP1	0.98
	ICAM-1	1.15		
Metabolites	Shikimate	0.49	*p*-Hydroxyphenylacetate	0.40
	CAR 18:1	0.60	CAR 18:1*	0.60
	CAR 18:0	0.64	CAR 18:0*	0.64
	CAR 18:2	0.75	CAR 18:2	0.75
	CAR 16:0	0.76	Succinate	0.80
	Isocitrate	0.78	Gluconolactone	0.84
	Lys	1.27	Lys*	1.27
	Oleate	1.40	Gly-pro*	2.03
	DHA	1.50	CAR 10:0	2.16
	CAR DC5:0	1.52	FA C19:1	3.32
	Undecylenate	1.87	Butyrate*	3.80
	5-Dodecenoate	1.93		
	Gly-pro	2.03		
	CAR 10:0	2.16		
	AMP	2.63		
	CAR 8:0	3.07		
	FA C19:1	3.32		
	Fumarate	3.42		
	Butyrate	3.80		
	CAR 6:0	9.52		

*The variables used in the classification of the CA and CO groups.

ICAM-1 in the CA group were 11.7 pg/mL and 10.8 ng/mL, respectively.

Furthermore, the cytokine signatures that were found in the plasma samples of the COVID-19 patients during hospitalization showed distinct patterns in the plasma samples of patients recovered from the disease (13, 14). Alone with the still higher levels of TNF, both IL-6 and MCP1, the other two cytokine markers, dramatically increased in COVID-19 patients, had similar levels across all three groups (Fig. 2*A* and *SI Appendix*, Fig. S1*E*). Also, some inflammatory cytokines were altered only in patients of the same gender. For example, the average concentration of IL-5 in healthy female subjects (42.4 pg/mL) differed from those in the CA females (124.3 pg/mL) and CO females (109.9 pg/mL) (Fig. 2*H*). Similarly, it was observed that MIP-1δ decreased only in the male convalescents in the CO group (Fig. 2*I*). These data indicate sex heterogeneity of immune responses in the convalescent patients with COVID-19.

Metabolomic Profiling of Convalescent COVID-19 Patients. As mentioned above, cytokine profiling reveals heterogeneities in convalescent COVID-19 patients including antibody fading-related and sex-specific cytokine patterns. We further asked whether metabolic heterogeneity could be delineated in convalescents. Therefore, to clarify the alterations in the plasma metabolome of convalescent COVID-19 patients especially that related to the various levels of the virus-specific antibodies, we profiled the small-molecular metabolites in the plasma sample sets of all three groups. Based on the fragment ions and retention times of standards, we quantified a total of 187 metabolites with each standard curve (*SI Appendix*, Fig. S2 and Table S3). As all were free of the disease on the day of sample collection, the subjects of three groups had only a slight difference in the overall profile of metabolome, indicating modest impacts of COVID-19 on plasma metabolome after recovery (Fig. 1*E* and *SI Appendix*, Fig. S2). The metabolomics data were also processed using ANCOVA with both sex and age as covariates to diminish the impacts of sex and age. As compared with the H group, alterations of 24 and 37 metabolites were found from the CA and CO groups, respectively (*SI Appendix*, Fig. S3). Between the CA and CO groups, 20 differential metabolites were highlighted (Table 1). Among all three groups, dipeptide gly-pro accumulated in both convalescent groups with the highest concentrations in the CO individuals (Fig. 3*A*). Moreover, the three acylcarnitines, stearylcarnitine (CAR 18:0), oleylcarnitine (CAR 18:1), and linoleylcarnitine (CAR 18:2), were lower in both convalescent groups with the lowest levels in the CO individuals (Fig. 3*B* and *SI Appendix*, Fig. S3). Interestingly, other long-chain acylcarnitines (CAR 14:0 and CAR 16:0), albeit less significantly, showed the same altered trend, while medium-chain acylcarnitines, CAR 6:0, CAR 8:0 and CAR 10:0, were mapped in an opposite pattern (*SI Appendix*, Fig. S3). By paying attention to the CO group, our results illuminated that several metabolites changed in the CO group when compared with the healthy subjects and/or CA individuals, such as the up-regulation of AMP (Fig. 3*C*) and docosahexaenoic acid (DHA) (*SI Appendix*, Fig. S3) and depletion of isocitrate (Fig. 3*D*). Also, we observed seven metabolites, such as lysine and butyrate, declined only in the CA group (Fig. 3 *E* and *F* and *SI Appendix*, Fig. S3).

The sex-specific metabolic signatures have also been delineated. Among the 134 metabolites that had no obvious difference

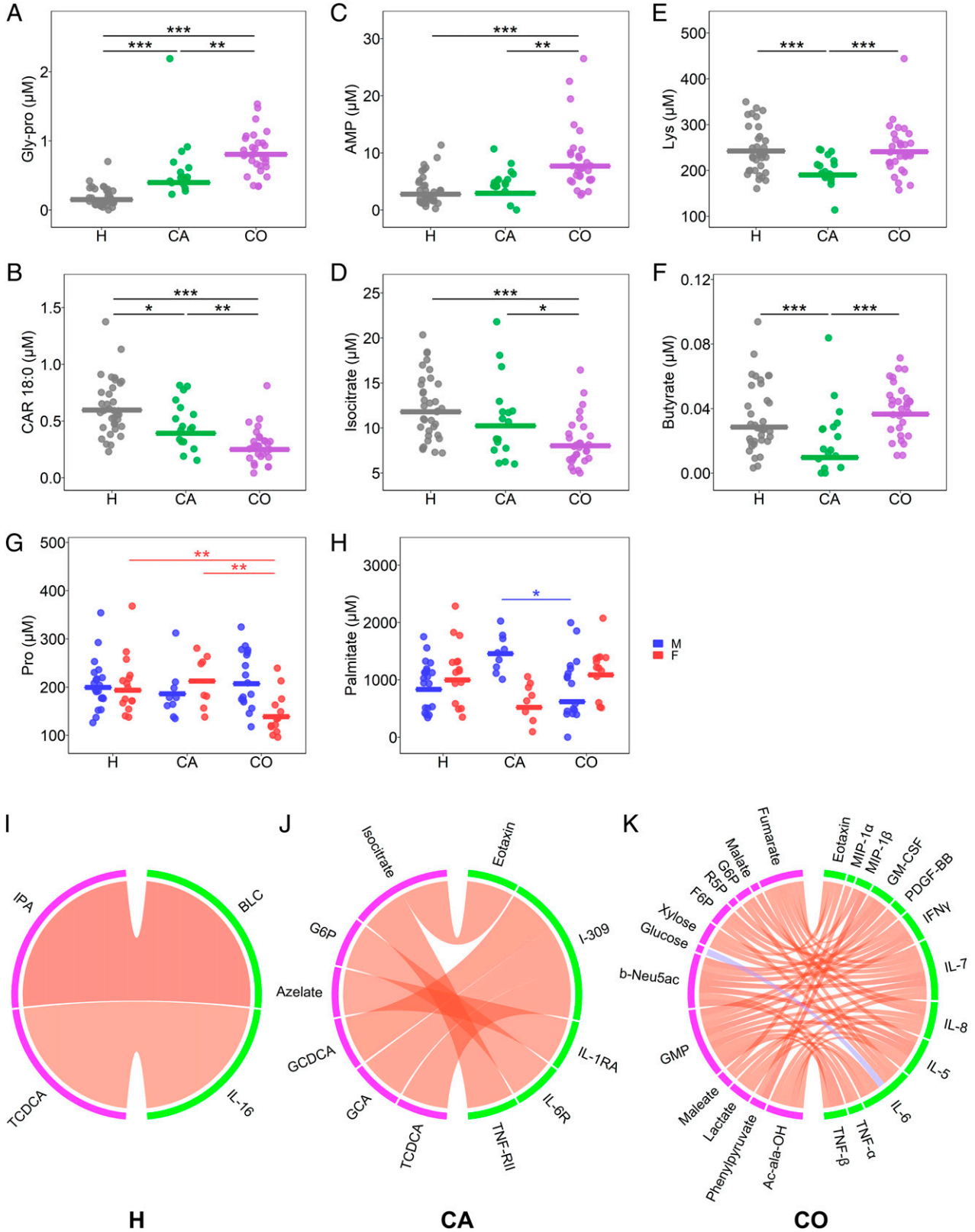

Fig. 3. The absolute quantification of the metabolome. (*A–F*) The representatives of the metabolites that showed significant alterations among the three groups, including gly-pro (*A*), CAR 18:0 (*B*), AMP (*C*), isocitrate (*D*), Lys (*E*), and butyrate (*F*). (*G* and *H*) The levels of Pro (*G*) and palmitate (*H*) that significantly changed only between the different groups of the male or female patients, respectively. (*I–K*) The highly correlated pairs (Pearson's correction coefficient >0.8 or <−0.8, $q < 0.1$) in the H (*I*), CA (*J*), and CO (*K*) groups. The red and blue lines annotate positive and negative correlations, respectively. The significance annotations in *A–H* are the same as those in Fig. 2.

between any two groups, 25 metabolites were found to be significant when the male and female subjects were compared separately, 16 only in the females, 8 only in the males, and 1 in both (*SI Appendix*, Fig. S4). The females had 17 metabolites of different levels between at least two groups, among which 11 showed to be significant between the CA and CO groups, such as

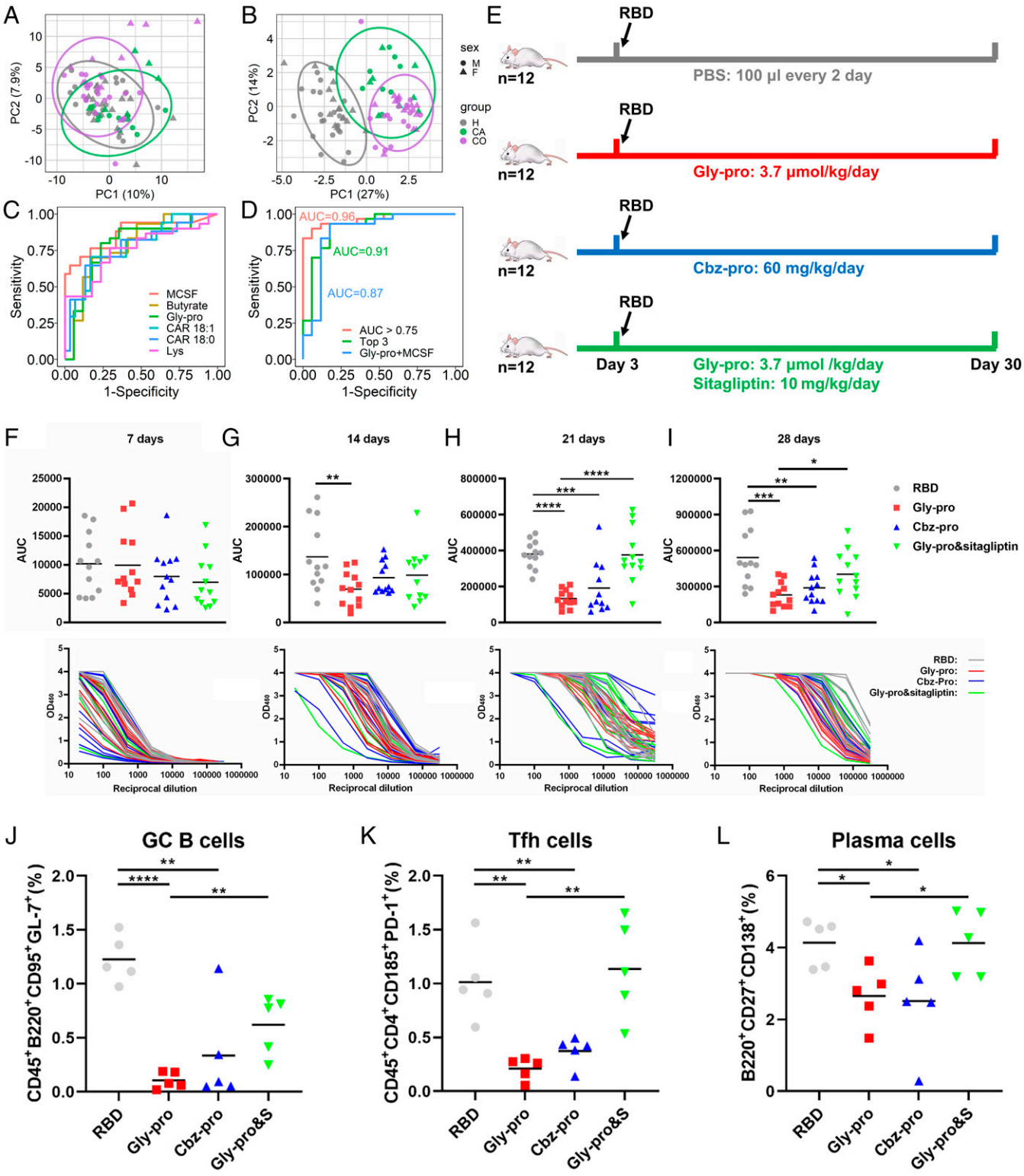

Fig. 4. The features selected for predicting the CO patients from the CA patients. (*A* and *B*) PCA of all 225 features measured (38 inflammatory factors and 187 metabolites, *A*) and the 17 selected features (6 cytokines and 11 metabolites, *B*). (*C*) The ROC curves of six features that showed the largest AUROC in discriminating the CA and CO groups. (*D*) The ROC curves of binomial logistic regression models using gly-pro and one, two, or five more features. (*E*) The schematic workflow of the RBD immunization experiment in a mouse model. (*F–I*) Serum IgG antibody against SARS-CoV-2 RBD domain was measured 1 (*F*), 2 (*G*), 3 (*H*), and 4 (*I*) wk postimmunization with RBD protein. The lower and upper panels show optical density at 450 nm (OD_{450}) readout curves from reciprocal dilution assay and the areas under the curves (AUC), respectively. (*J–L*) Detection of GC B cells (*J*), Tfh cells (*K*) and plasma cells (*L*) in the immunized mouse lymph nodes (for Tfh and GC-B cells) and spleens (for plasma cells). Frequencies of GC B ($CD45^+B220^+CD95^+GL\text{-}7^+$), Tfh ($CD45^+CD4^+CD185^+PD\text{-}1^+$), and plasma ($B220^+CD27^+CD138^+$) cells were analyzed by flow cytometry. Data are presented as mean ± SEM of mice ($n = 5$ per group). $^*P < 0.05$; $^{**}P < 0.01$; $^{****}P < 0.0001$. Gly-pro: glycylproline; Gly-pro&S: combined treatment with glycylproline and sitagliptin; Cbz-pro: *N*-benzyloxycarbony-L-proline.

declined proline and 4-hydroxyphenylpyruvic acid in the female CO group (Fig. 3*G* and *SI Appendix*, Fig. S4). Among the nine metabolites that were altered in the males, most of them (eight metabolites) including palmitate showed significant changes between the male CA and CO individuals (Fig. 3*H*). Moreover, higher levels of palmitate and creatine in females compared with

males (*SI Appendix*, Fig. S5*A*) and higher levels of 28 other metabolites in males compared with females (*SI Appendix*, Fig. S5*B*) were observed in the CO group, mapping sex-specific metabolic signatures in the CO individuals. Taken together, these obtained results further evidenced the role of sex in the immunometabolism responses to SARS-CoV-2 infection, which needs further exploration.

Correlation between Cytokines and Metabolites of Convalescent COVID-19 Patients. To further check if the changes in the profiles of cytokines and plasma metabolites are associated with the onset of COVID-19, we calculated the Pearson's correlation between each cytokine and each metabolite across all individuals of the same groups. As a result, Pearson's correlation coefficients (PCC) defined only many more pairs of correlation (PCC > 0.8 or < -0.8, and $q < 0.1$) in the CO group compared with that in the H group or even the CA group (Fig. 3 *I*–*K*). The poor correlation between inflammatory cytokines and metabolites suggests that the differences of these molecules across all persons are mostly individual variance (Fig. 3*I*). On the other hand, lots of highly correlated pairs existed in the convalescent groups, indicating the infection of SARS-CoV-2 changed the immune system of the host to a certain extent even after their recovery from COVID-19 (Fig. 3 *J* and *K*). The CO group had a number of correlated pairs between 12 inflammatory factors and 13 metabolites, forming a complex network (Fig. 3*K*). Intriguingly, none of these correlations existed in the CA patients. IFNγ is an indicator of COVID-19 and increased in both CA and CO groups (Fig. 2*C*). The plasma IFNγ was correlated with GMP (*SI Appendix*, Fig. S6*A*), b-Neu5Ac (*SI Appendix*, Fig. S6*B*), and R5P (*SI Appendix*, Fig. S6*C*) in the CO group but not in the CA group. So did other inflammatory cytokines, such as GM-CSF (*SI Appendix*, Fig. S6 *D* and *E*) and MIP-1a (*SI Appendix*, Fig. S6*F*). The correlations between these cytokines and certain metabolites were observed only from the CO group. Together, more correlations between the metabolic signatures and inflammatory cytokines are associated with the rapid fading of antibodies in the COVID-19 convalescents.

Machine-Learning Models for Classification. Due to the capacity of cytokine profiling and metabolomics analysis, the number of measured molecules was much larger than that of samples. To determine if the machine-learning approaches can facilitate classifying patients based on the molecular characteristics, we conducted the least absolute shrinkage and selection operator (LASSO) to select the features from both cytokines and metabolites to avoid overfitting to the limited number of samples. Regarding the discrepancies in the age and sex composition of the cohort, we first applied a three-way ANOVA to find the variables that were significantly affected by the factors age and sex or interactions involving these two factors. After removing these cytokines and metabolites, 187 variables (13 cytokines and 174 metabolites) were included in the following feature selection. Also, because the feature selection can generally be unstable in small datasets, the regularization penalty λ, the hyperparameter of LASSO, was determined based on the misclassification error (MCE) averaged from 10,000 times of random fivefold cross-validation using multinomial logistical regression (MLR) (*SI Appendix*, Fig. S7). The most regularized model within one SE of the minimum MCE gave 17 features, including 6 inflammatory factors, Eotaxin, M-CSF, IL-6R, IL-12p40, TIMP1, and TIMP2, and 11 metabolites, gly-pro, Lys, butyrate, succinate, *p*-hydroxyphenylacetate, gluconolactone, decanoylcarnitine (CAR 10:0), CAR 18:0, CAR 18:1, CAR 18:2, and fatty acid (C19:1) (Table 1). Thereby, these 17 features were used as potential biomarkers to discriminate the convalescent patients with or without antibodies from healthy subjects.

Principal component analysis (PCA) results utilizing all measured cytokines and metabolites (Fig. 4*A*) and only the 17 selected ones (Fig. 4*B*) demonstrated that the variance of these selected features among individuals reflected more diversities between groups. Based on these 17 selected features, all fivefold cross-validations using various machine-learning methods, including neural network (*SI Appendix*, Fig. S8*A*), support vector machine (*SI Appendix*, Fig. S8*B*), ensemble of subspace discriminant (*SI Appendix*, Fig. S8*C*), linear discriminant analysis (*SI Appendix*, Fig. S8*D*), random forest (*SI Appendix*, Fig. S8*E*), and k-nearest neighbors (*SI Appendix*, Fig. S8*F*), on these 17 selected features all resulted in a prediction of over 90% accuracy. As shown in both PCA clusters and machine-learning results, the two subgroups of convalescents were more similar to each other and harder to distinguish. To further improve the prediction power for the CA and CO groups, we calculated the area under the receiver operating characteristic (AUROC) for each of these features. The six features that had significant differences between the CA and CO groups and had an AUROC of greater than 0.75 in clustering the convalescent patients (Fig. 4*C*) were further selected from the 17 ones to classify these two groups. A binomial logistic regression model using these six features provides a predictor of AUROC 0.96 (Fig. 4*D*). Using only the three features of the highest AUROC, gly-pro, M-CSF, and butyrate, the performance was still 0.91. If only the most contributing metabolites gly-pro and the cytokine M-CSF in the model (*SI Appendix*, Fig. S9) were used, an AUROC near 0.9 was also achieved (Fig. 4*D*). The obtained results highlight that the specific metabolic markers and inflammatory responses are associated with antibody fading in convalescent patients with COVID-19.

Role of gly-pro and DPP4 in SARS-CoV-2 RBD Antibody Production. As aforementioned, in the quantitative metabolome we specifically identified that one dipeptide, gly-pro, had the largest increases (2.5-fold in CA and 4.0-fold in CO) in both convalescent groups compared with healthy subjects (Fig. 3*A*). This molecule is likely the product of DPP4 protein, which cuts the N-terminal dipeptide from polypeptides. DPP4 is widely expressed in various types of immune cells and capable of modulating plenty of inflammatory cytokines (25). It has been demonstrated that DPP4 is the functional receptor of MERS-CoV, the coronavirus causing Middle East respiratory syndrome (26). Previous studies have reported the interaction between DPP4 and the spike glycoprotein SARS-CoV-2 and the coreceptor role of DPP4 in viral entry (27, 28). Also, in independent clinical trials the use of DPP4 inhibitors reduced the mortality of COVID-19 patients (20–22). DPP4 inhibitors have been used for years in the clinical treatment of patients with type 2 diabetes (29), which is also one of the well-known risk factors for adverse outcomes of COVID-19 (30). To interrogate whether gly-pro and DPP4 have functional roles in the production of antibodies against SARS-CoV-2, we conducted an RBD immunization experiment in mice. Four groups of female mice were intraperitoneally injected with 50 μg of SARS-CoV-2 RBD when 6 wk old (Fig. 4*E*). Exogenous gly-pro was supplied to one group (the Gly-pro group), and we also applied *N*-benzyloxycarbony-L-proline (Cbz-pro), the inhibitor of the proline dipeptidase prolidase that degrades gly-pro (31), to a group of mice to block the degradation of endogenous gly-pro (the Cbz-pro group). Another

group was cotreated with gly-pro and the DPP4 inhibitor sitagliptin (the gly-pro & sitagliptin group). The control group was injected with phosphate-buffered saline (PBS) (the PBS group). All mice had been monitored for 4 wk since single-dose immunization and serum IgG antibodies against the RBD domain were measured weekly. During the immunization experiment, no significant difference in the body weight of all animals was observed (*SI Appendix*, Fig. S10). One week after the immunization, the serum antibody levels of the four groups were similar (Fig. 4*F*). Since the second week, the gly-pro group showed a lower level of IgG specific to the SARS-CoV-2 RBD (Fig. 4 *G*–*I*). The inhibition of its degradation (i.e., the Cbz-pro group) also led to a significant decrease in the antibodies after 3 wk (Fig. 4*H*). On the other hand, inhibition of the activity of DPP4 at least partially rescued the suppressed antibody production caused by gly-pro (Fig. 4 *G*–*I*).

Because the germinal center (GC) response takes at least one to several weeks to mature and GC B cells with higher affinity can uptake and present antigen more efficiently to T follicular helper cells (Tfh), meanwhile, as the part of the memory compartment of B cells, long-lived plasma cells can be differentiated from GC B cells (32, 33). Herein, to further explore the changes in immune responses caused by Gly-pro, we carried out the flow cytometry gating strategy for the identification of GC B cells ($CD45^+B220^+CD95^+GL\text{-}7^+$), Tfh cells ($CD45^+CD4^+CD185^+PD\text{-}1^+$), and plasma cells ($B220^+CD27^+CD138^+$) (*SI Appendix*, Fig. S11). As a result, the flow cytometry sorting data demonstrated that both exogenous supply (i.e., the Gly-pro group) and endogenous accumulation of gly-pro by the Cbz-pro treatment can reduce the generation of immune cells in response to SARS-CoV-2 RBD immunization, including GC B cells (Fig. 4*J*), Tfh cells (Fig. 4*K*), and plasma cells (Fig. 4*L*). Moreover, inhibiting DPP4, an enzyme catalyzing to form gly-pro, counteracted the down-regulated immune cells caused by the dipeptide (Fig. 4 *J*–*L* and *SI Appendix*, Fig. S11). Taken together, SARS-CoV-2 RBD antibody production can be regulated by gly-pro supplement and/or its producing protein DPP4, suggesting that modulation of antibody levels could be an important approach in physiological conditions for vaccination.

Discussion

The intraindividual variability in the production and decay of antibodies in response to the virus and vaccines of SARS-CoV-2 has been well-documented, but the mechanism underlying this heterogeneity is poorly understood. The present study conducted absolute quantification of both cytokines and metabolites in the plasma sample sets of convalescent COVID-19 patients with (the CA group) and without (the CO group) the virus-specific antibodies. After recovery from the disease, the plasma metabolomes of both groups were highly similar to those from healthy persons, except for a few metabolite markers (Fig. 1*E* and *SI Appendix*, Fig. S2). However, the plasma inflammatory cytokines of these convalescent individuals still kept clear "memories" of the onset of COVID-19 (Fig. 1*E*). The cytokines of antiviral function, such as IFNγ (34) and TNF (35), which were up-regulated in the blood of COVID-19 patients (14), were still higher in both groups of convalescents (Fig. 2 *B* and *C* and *SI Appendix*, Fig. S1). IL-6 has been associated with severe COVID-19 symptoms and a poor prognosis. However, in these convalescents, the level of IL-6 was as same as that in the healthy people (*SI Appendix*, Fig. S1*E*). The lower level of IL-6R (*SI Appendix*, Fig. S1*B*) was likely related to the recovery of these patients. A similar case is the plasma levels of the TNF-α receptor TNF-RII. The increased soluble TNF-α receptor has been proposed as an indicator of higher intensive care unit mortality of COVID-19 (36). Together with cytokine storm, the main cause of fatality in COVID-19 patients (14, 15), the lower levels of these cytokine receptors were possibly the reasons for their survival. As compared with the CA group, the even lower level of TNF-RII in the CO patients (*SI Appendix*, Fig. S1*B*) might be associated with a milder immune response and rapid fading of the virus-specific antibodies. In particular, IL-12p40 has the most down-regulated level in the CO individuals compared with that in the CA and healthy groups (Fig. 2*D*). It is well known that IL-12p40 is a component of the bioactive cytokines IL-12 and IL-23, acting as a chemoattractant for macrophages and promoting the migration of dendritic cells for pathogenic inflammatory responses (37), indicating that inflammation may be associated with antibody immunity in convalescents against SARS-CoV-2 infection.

To further identify the biomarkers from the plasma samples of convalescent patients, the application of LASSO using MLR facilitated the determination of a minimal number of features that can distinguish the three groups of samples. The classification results from various machine-learning algorithms (*SI Appendix*, Fig. S8) demonstrated the great potential of these molecules in both basic research and clinical applications. Among them, the six molecules that were selected to classify the CA and CO groups (Fig. 4*C* and Table 1), especially gly-pro, are of value in the prognosis of COVID-19 and prediction of vaccination efficiency (Fig. 4). It should be noted that we applied ANOVA and excluded the variables (i.e., cytokines or metabolites) that showed significant alterations with age and sex before LASSO feature selection. These data processing steps were largely responsible for the discovery of these valuable biomarkers in the cohort of disparate composition. More importantly, the fact that no significant difference in the positive days of convalescent patients (Fig. 1*D*) further supports that the biomarkers (6 cytokines and 11 metabolites) can reveal the molecular characteristics in either the CA or CO individuals discriminating from healthy subjects upon SARS-CoV-2 infection.

Due to cytokine features as the biomarkers, we further focused on the metabolic regulation in antibody immunity by gly-pro, the most accumulated metabolite in the CO individuals (Fig. 3*A*). The antibody response assay in the mouse model has validated the role of gly-pro in the production of antibodies against the RBD domain of SARS-CoV-2 (Fig. 4). Increasing gly-pro via exogenous supply or inhibiting its digesting enzyme with Cbz-pro treatment resulted in a lower SARS-CoV-2 RBD-specific antibody level. The pharmaceutical inhibition of DPP4, the producing enzyme of gly-pro, rescued the adverse impacts of gly-pro on antibody production (Fig. 4). Further confirmation in GC B, Tfh, and plasma cells of the vaccinated mice indicated that gly-pro supplement can suppress antibody immunity whereas sitagliptin can at least partially counteract the inhibitory effects of gly-pro on RBD antibody production in mice, supporting our notion that DPP4 inhibitors might be the therapeutic potentials for maintaining neutralizing antibody levels.

DPP4 is an aminopeptidase expressed in various cell types and interacting with a wide range of proteins, including peptide hormones, chemokines, and immunomodulatory proteins (38). Due to its function of degradation incretins, DPP4 has been associated with diabetes and obesity, the most reported comorbidities linked to the severity of COVID-19 (39–41). It also functions in the immune response by digesting chemokines such as CXCL10 (42) and by forming a complex with other immunoregulatory proteins like adenosine deaminase (43). This protein is a receptor of MERS-CoV, another coronavirus that can cause severe respiratory disease (26). Its role in the

course of COVID-19 still attracts a lot of attention and needs to be clarified. On the one hand, previous studies have demonstrated that DPP4 is not essential for the cellular entry of SARS-CoV-2. However, three clinical trials independently conducted in Italy (21) and Korea (22) consistently reported that the applications of DPP4 inhibitors significantly reduced the rates of severity and mortality of COVID-19 patients with type 2 diabetes. Regarding the multifunction of this enzyme, various possible functional routes from DPP4 or DPP4 inhibitors to COVID-19 have been proposed (38). By demonstrating the role of gly-pro, one of the DPP4 products, in the production of SARS-CoV-2 antibodies, our results provide a possible mechanism underlying the clinical efficacy of DPP4 inhibitors in COVID-19 treatment. An increase in DPP4 has been associated with diabetes and DPP4 inhibition is a widely used strategy in the treatment of type 2 diabetes mellitus (44). A recent vaccination study on diabetic patients reported lower SARS-CoV-2 IgG and neutralizing antibody titers in persons with type 2 diabetes (45). Thus, our results have also provided us deeper insights into how the comorbid condition of diabetes mellitus influences the severity of this infectious disease. Furthermore, our finding showed that gly-pro could modulate the immune response to the SARS-CoV-2 RBD vaccine. This direction effect has provided a new target for intervention, which might help avoid the possible side effects of overweight and immune suppression caused by DPP4 inhibitors. It should be noted that no convalescent patients with diabetes were enrolled in our study, suggesting that gly-pro plays a critical role in antibody immunity against SARS-CoV-2 infection.

Besides gly-pro, only a small proportion of measured metabolites showed significant alterations between various groups of plasmas. The elevated AMP level was found in both the CA (1.4-fold) and CO (2.5-fold) groups (Fig. 3*C*), indicating an increase in energy demand in the recovered patients. Accordingly, the intermediates of the citric acid cycle (TCA cycle), isocitrate and succinate, decreased in both the CA (−1.1- and −1.2-fold, respectively) and CO (−1.5- and −1.6-fold, respectively) groups (Fig. 3*D* and *SI Appendix*, Fig. S3). The reduced levels of plasma of acylcarnitines observed in both convalescent groups are consistent with this trend (Fig. 3*B* and *SI Appendix*, Fig. S3). These data suggested that to meet this raised demand for energy the convalescents might up-regulate the fatty acid β-oxidation pathway, an alternative pathway for energy supply (46, 47). One of the best-known concepts in immunology is that the immune response activities, such as fever, generating new immune cells, and producing antibodies require high levels of energy. Intriguingly, although both altered consistently, the changes of these molecules reached higher extents in the CO group, indicating a larger energy gap in the convalescents of fading antibodies. It is worth further study to clarify if the shortage in energy supply is a reason for the rapid decrease of antibody production. Our results of the correlation between inflammatory factors and metabolites also support this speculation. The CO group had the largest number of inflammatory factor–metabolite pairs of strong correlation (Fig. 3*K*). The 13 metabolites correlated to one or more cytokines include carbon sources glucose and lactate and the intermediates of the central metabolic pathway such as F6P, G6P, xylose, R5P, fumarate, and malate. The positive correlation between these metabolites possibly indicates that central metabolism is the rate-limited pathway for the production of these cytokines. Among the pairs, the only negatively correlated pair is glucose and IL-6 (Fig. 3*K*). Glucose is the main energy source of most cells, and IL-6 is one of the characteristic cytokines in COVID-19. The negative correlation might result from the consumption of glucose by the immune response. Moreover, a recent study demonstrated that DPP4 inhibition increases the levels of inflammatory markers in the plasma of regular-chow-fed mice but not that of high-fat-fed ones (48), further supporting the importance of energy supply in the systematic immune response to COVID-19.

It has been noticed since the start of the pandemic that males are more vulnerable to COVID-19 than females in terms of both morbidity and mortality across all ages (49). This is genetically sound because some essential proteins in SARS-CoV-2 infections are encoded by the X chromosome genes. These genes include angiotensin-converting enzyme 2 (ACE2), a cell-entry receptor of the virus (50), and Toll-like receptor 7 (TLR7), a lung-abundant receptor recognizing viral RNA to produce type 1 interferon (51, 52). The clinical samples of male and female COVID-19 patients have revealed that the males had higher levels of IL-8 and CCL5 in their plasma and change in some cytokines, such as TNFSF10 and IL-15, was associated with severity only in the female group (53). The sex difference has also been observed from our data of convalescent patients. In addition, more sex difference has been quantified from the metabolites (*SI Appendix*, Fig. S4). The 30 metabolites of varying levels only in the CO group but not the H group are probably correlated with the sex difference in the immune response to SARS-CoV-2 (*SI Appendix*, Fig. S5). Overall, sex-specific antibody immunity against the infections of SARS-CoV-2 wild type as well as variants still requires further exploration.

Materials and Methods

Ethics and Patient Samples. All studies performed in the present work were approved by the Wuhan Jinyintan Hospital Ethics Committee (no. KY-2020-83) and written informed consents were obtained from patients. All SARS-CoV-2 cases were diagnosed based on RT-PCR analysis of viral RNA. The severity of COVID-19 was determined by the attending doctors based on the clinical diagnostic guidelines of the Chinese Health Commission (sixth edition). The blood samples of the convalescent patients (both the CA and CO groups) were collected at 40∼70 d after the confirmation of COVID-19 onset. All patients had been cured and discharged before the sample collection. No diabetic person was included in the cohort. All blood samples were collected after fasting overnight and by potassium–ethylenediaminetetraacetic acid blood collection tubes. The anti–SARS-CoV-2 IgG was detected with RBD IgG enzyme-linked immunosorbent assay ELISA kits (Wuhan anbo Bio Co., Ltd) following the manufacturer's instructions (*SI Appendix*).

Absolute Quantification and Analysis of Inflammatory Factors and Metabolome in Plasmas. Plasmas were separated from all blood samples by centrifugation. The inflammatory factors were quantified using the All Human Inflammation Array Q3 kit (RayBiotech Life, Inc.) and metabolites were absolutely quantified by using Q300 Kit (Metabo-Profile) and QTRAP 6500+ triple quadrupole mass spectrometer (SCIEX). The data were processed using R language with R packages STATS, RSTATIX, EMMEANS, and ROPLS. The features selection with LASSO was performed with the GLMNET package. Machine learning is conducted with machine learning applications of MATLAB (version R2018b; MathWorks). See *SI Appendix* for the details.

Mouse Immunization, Serum Antibody Measurement, and Flow Cytometry. The recombinant RBD of the spike protein of SARS-CoV-2 was a kind gift of Prof. Xiao Gengfu, Wuhan Institute of Virology, Wuhan, China. The purified recombinant RBD protein was mixed with Freund's incomplete adjuvant (Sigma-Aldrich). Four groups (12 mice each) of 6-wk-old female mice were injected with recombinant RBD intramuscularly, 25 μg per mouse. The mice were daily treated intraperitoneally with PBS, 3.7μmol/kg gly-pro, 60 mg/kg Cbz-pro, and 3.7μmol/kg Gly-pro plus 10 mg/kg sitagliptin. Blood sera were collected from retroorbital puncture at 7, 14, 21, and 28 d postimmunization and total IgG antibodies against the RBD domain of SARS-CoV-2 were measured with reciprocal dilution assay. Two weeks postimmunization, the lymph nodes were

collected for the analysis of GC B and Tfh cells, and the spleens were collected for the analysis of plasma cells. The cell populations were analyzed with fluorescence activated cell sorting (FACS; Becton Dickinson) using fluorophore-conjugated monoclonal antibodies specific to each cell type. See *SI Appendix* for the details. All studies involving mice were approved by the Animal Care and Use Committee of Wuhan Institute of Virology.

Data Availability. The mass spectrometry data for metabolomics have been deposited at Metabolomics Workbench (https://www.metabolomicsworkbench.org/), and are accessible with the identifier ST001933 (54). All other study data are included in the article and/or supporting information.

ACKNOWLEDGMENTS. This work was funded by the National Natural Science Foundation of China (Grants 91957120 and 21974114 to S.-H.L., Grant 92169107 to D.-Y.Z., and Grant 32000131 to D.W.), the Fundamental Research Funds for the Central Universities (Grants 20720220003 and 20720210001 to S.-H.L.), and the University Grants Committee (Grant 12103820 to Z.Y., and Grants T11-709/21-N and C7042-21G to Z.C.).

Author affiliations: [a]State Key Laboratory for Cellular Stress Biology, School of Life Sciences, Faculty of Medicine and Life Sciences, Xiamen University, Fujian 361102, China; [b]National Institute for Data Science in Health and Medicine, Xiamen University, Fujian 361102, China; [c]State Key Laboratory of Environmental and Biological Analysis, Department of Chemistry, Hong Kong Baptist University, Hong Kong SAR, China; [d]State Key Laboratory of Virology, Wuhan Institute of Virology, Center for Biosafety Mega-Science, Chinese Academy of Sciences, Wuhan 430071, China; [e]Joint Laboratory of Infectious Diseases and Health, Wuhan Institute of Virology–Wuhan Jinyintan Hospital, Wuhan 430023, China; [f]Center for Translational Medicine, Jinyintan Hospital, Wuhan 430023, China; and [g]Department of Critical Care Medicine, Union Hospital, Tongji Medical College, Huazhong University of Science and Technology, Wuhan 430030, China

Author contributions: Y.Q., D.-Y.Z., X.Z., Y.S., and S.-H.L. designed research; Z.Y., D.W., S.L., Z.H., F.T., C.Z., and L.Z. performed research; Z.Y., D.W., S.L., and S.-H.L. analyzed data; and Z.Y., Y.Q., X.Z., Z.C., Y.S., and S.-H.L. wrote the paper.

The authors declare no competing interest.

1. A. Wu *et al.*, Genome composition and divergence of the novel coronavirus (2019-nCoV) originating in China. *Cell Host Microbe* **27**, 325–328 (2020).
2. N. L. Pereira *et al.*, COVID-19: Understanding inter-individual variability and implications for precision medicine. *Mayo Clin. Proc.* **96**, 446–463 (2021).
3. D. F. Gudbjartsson *et al.*, Humoral immune response to SARS-CoV-2 in Iceland. *N. Engl. J. Med.* **383**, 1724–1734 (2020).
4. J. Zhao *et al.*, Antibody responses to SARS-CoV-2 in patients of novel coronavirus disease 2019. *Clin. Infect. Dis.* **71**, 2027–2034 (2020).
5. Q. X. Long *et al.*, Clinical and immunological assessment of asymptomatic SARS-CoV-2 infections. *Nat. Med.* **26**, 1200–1204 (2020).
6. P. M. Folegatti *et al.*; Oxford COVID Vaccine Trial Group, Safety and immunogenicity of the ChAdOx1 nCoV-19 vaccine against SARS-CoV-2: A preliminary report of a phase 1/2, single-blind, randomised controlled trial. *Lancet* **396**, 467–478 (2020).
7. C. Keech *et al.*, Phase 1-2 trial of a SARS-CoV-2 recombinant spike protein nanoparticle vaccine. *N. Engl. J. Med.* **383**, 2320–2332 (2020).
8. F. C. Zhu *et al.*, Immunogenicity and safety of a recombinant adenovirus type-5-vectored COVID-19 vaccine in healthy adults aged 18 years or older: A randomised, double-blind, placebo-controlled, phase 2 trial. *Lancet* **396**, 479–488 (2020).
9. S. Xia *et al.*, Effect of an inactivated vaccine against SARS-CoV-2 on safety and immunogenicity outcomes: Interim analysis of 2 randomized clinical trials. *JAMA* **324**, 951–960 (2020).
10. H. Pan *et al.*, Immunogenicity and safety of a third dose, and immune persistence of CoronaVac vaccine in healthy adults aged 18-59 years: Interim results from a double-blind, randomized, placebo-controlled phase 2 clinical trial. *Medrxiv*, 2021.07.23.21261026 (2021).
11. D. S. Khoury *et al.*, Neutralizing antibody levels are highly predictive of immune protection from symptomatic SARS-CoV-2 infection. *Nat. Med.* **27**, 1205–1211 (2021).
12. N. Kaneko *et al.*; Massachusetts Consortium on Pathogen Readiness Specimen Working Group, Loss of Bcl-6-expressing T follicular helper cells and germinal centers in COVID-19. *Cell* **183**, 143–157.e13 (2020).
13. T. Chen *et al.*, Clinical characteristics of 113 deceased patients with coronavirus disease 2019: Retrospective study. *BMJ* **368**, m1091 (2020).
14. C. Huang *et al.*, Clinical features of patients infected with 2019 novel coronavirus in Wuhan, China. *Lancet* **395**, 497–506 (2020).
15. P. Mehta *et al.*; HLH Across Speciality Collaboration, UK, COVID-19: Consider cytokine storm syndromes and immunosuppression. *Lancet* **395**, 1033–1034 (2020).
16. B. Shen *et al.*, Proteomic and metabolomic characterization of COVID-19 patient sera. *Cell* **182**, 59–72.e15 (2020).
17. D. Wu *et al.*, Plasma metabolomic and lipidomic alterations associated with COVID-19. *Natl. Sci. Rev.* **7**, 1157–1168 (2020).
18. N. Xiao *et al.*, Integrated cytokine and metabolite analysis reveals immunometabolic reprogramming in COVID-19 patients with therapeutic implications. *Nat. Commun.* **12**, 1618 (2021).
19. L. Zhu *et al.*, Association of blood glucose control and outcomes in patients with COVID-19 and pre-existing Type 2 diabetes. *Cell Metab.* **31**, 1068–1077.e3 (2020).
20. M. Mirani *et al.*, Impact of comorbidities and glycemia at admission and dipeptidyl peptidase 4 inhibitors in patients with type 2 diabetes with COVID-19: A case series from an Academic Hospital in Lombardy, Italy. *Diabetes Care* **43**, 3042–3049 (2020).
21. S. B. Solerte *et al.*, Sitagliptin treatment at the time of hospitalization was associated with reduced mortality in patients with type 2 diabetes and COVID-19: A multicenter, case-control, retrospective, observational study. *Diabetes Care* **43**, 2999–3006 (2020).
22. Y. Noh *et al.*, Association between DPP-4 inhibitors and COVID-19-related outcomes among patients with type 2 diabetes. *Diabetes Care* **44**, e64–e66 (2021).
23. N. Bar *et al.*; IMI DIRECT Consortium, A reference map of potential determinants for the human serum metabolome. *Nature* **588**, 135–140 (2020).
24. D. M. Del Valle *et al.*, An inflammatory cytokine signature predicts COVID-19 severity and survival. *Nat. Med.* **26**, 1636–1643 (2020).
25. S. Shao, Q. Xu, X. Yu, R. Pan, Y. Chen, Dipeptidyl peptidase 4 inhibitors and their potential immune modulatory functions. *Pharmacol. Ther.* **209**, 107503 (2020).
26. V. S. Raj *et al.*, Dipeptidyl peptidase 4 is a functional receptor for the emerging human coronavirus-EMC. *Nature* **495**, 251–254 (2013).
27. N. Vankadari, J. A. Wilce, Emerging WuHan (COVID-19) coronavirus: Glycan shield and structure prediction of spike glycoprotein and its interaction with human CD26. *Emerg. Microbes Infect.* **9**, 601–604 (2020).
28. F. Qi, S. Qian, S. Zhang, Z. Zhang, Single cell RNA sequencing of 13 human tissues identify cell types and receptors of human coronaviruses. *Biochem. Biophys. Res. Commun.* **526**, 135–140 (2020).
29. S. L. Zheng *et al.*, Association between use of sodium-glucose cotransporter 2 inhibitors, glucagon-like peptide 1 agonists, and dipeptidyl peptidase 4 inhibitors with all-cause mortality in patients with type 2 diabetes: A systematic review and meta-analysis. *JAMA* **319**, 1580–1591 (2018).
30. N. Chen *et al.*, Epidemiological and clinical characteristics of 99 cases of 2019 novel coronavirus pneumonia in Wuhan, China: A descriptive study. *Lancet* **395**, 507–513 (2020).
31. I. Myara, C. Charpentier, A. Lemonnier, Optimal conditions for prolidase assay by proline colorimetric determination: Application to iminodipeptiduria. *Clin. Chim. Acta* **125**, 193–205 (1982).
32. W. Luo, Q. Yin, B cell response to vaccination. *Immunol. Invest.* **50**, 780–801 (2021).
33. W. Tai *et al.*, A novel receptor-binding domain (RBD)-based mRNA vaccine against SARS-CoV-2. *Cell Res.* **30**, 932–935 (2020).
34. K. Schroder, P. J. Hertzog, T. Ravasi, D. A. Hume, Interferon-γ: An overview of signals, mechanisms and functions. *J. Leukoc. Biol.* **75**, 163–189 (2004).
35. R. M. Locksley, N. Killeen, M. J. Lenardo, The TNF and TNF receptor superfamilies: Integrating mammalian biology. *Cell* **104**, 487–501 (2001).
36. E. Mortaz *et al.*, Increased serum levels of soluble TNF-α receptor is associated with ICU mortality in COVID-19 patients. *Front. Immunol.* **12**, 592727 (2021).
37. A. M. Cooper, S. A. Khader, IL-12p40: An inherently agonistic cytokine. *Trends Immunol.* **28**, 33–38 (2007).
38. A. Krejner-Bienias, K. Grzela, T. Grzela, DPP4 inhibitors and COVID-19-holy grail or another dead end? *Arch. Immunol. Ther. Exp. (Warsz.)* **69**, 1 (2021).
39. Y. Cen *et al.*, Risk factors for disease progression in patients with mild to moderate coronavirus disease 2019-a multi-centre observational study. *Clin. Microbiol. Infect.* **26**, 1242–1247 (2020).
40. J. Yang *et al.*, Prevalence of comorbidities and its effects in patients infected with SARS-CoV-2: A systematic review and meta-analysis. *Int. J. Infect. Dis.* **94**, 91–95 (2020).
41. L. Roncon, M. Zuin, G. Rigatelli, G. Zuliani, Diabetic patients with COVID-19 infection are at higher risk of ICU admission and poor short-term outcome. *J. Clin. Virol.* **127**, 104354 (2020).
42. M. F. Bassendine, S. H. Bridge, G. W. McCaughan, M. D. Gorrell, COVID-19 and comorbidities: A role for dipeptidyl peptidase 4 (DPP4) in disease severity? *J. Diabetes* **12**, 649–658 (2020).
43. D. Röhrborn, N. Wronkowitz, J. Eckel, DPP4 in diabetes. *Front. Immunol.* **6**, 386 (2015).
44. B. Gallwitz, Clinical use of DPP-4 inhibitors. *Front. Endocrinol.* **10**, 389 (2019).
45. H. Ali *et al.*, Robust antibody levels in both diabetic and non-diabetic individuals after BNT162b2 mRNA COVID-19 vaccination. *Front. Immunol.* **12**, 752233 (2021).
46. R. J. A. Wanders, J. Komen, S. Kemp, Fatty acid omega-oxidation as a rescue pathway for fatty acid oxidation disorders in humans. *FEBS J.* **278**, 182–194 (2011).
47. R. Zechner *et al.*, FAT SIGNALS–Lipases and lipolysis in lipid metabolism and signaling. *Cell Metab.* **15**, 279–291 (2012).
48. L. L. Baggio *et al.*, Plasma levels of DPP4 activity and sDPP4 are dissociated from inflammation in mice and humans. *Nat. Commun.* **11**, 3766 (2020).
49. E. P. Scully, J. Haverfield, R. L. Ursin, C. Tannenbaum, S. L. Klein, Considering how biological sex impacts immune responses and COVID-19 outcomes. *Nat. Rev. Immunol.* **20**, 442–447 (2020).
50. J. Shang *et al.*, Cell entry mechanisms of SARS-CoV-2. *Proc. Natl. Acad. Sci. U.S.A.* **117**, 11727–11734 (2020).
51. S. S. Diebold, T. Kaisho, H. Hemmi, S. Akira, C. Reis e Sousa, Innate antiviral responses by means of TLR7-mediated recognition of single-stranded RNA. *Science* **303**, 1529–1531 (2004).
52. J. Di Domizio *et al.*, TLR7 stimulation in human plasmacytoid dendritic cells leads to the induction of early IFN-inducible genes in the absence of type I IFN. *Blood* **114**, 1794–1802 (2009).
53. T. Takahashi *et al.*, Sex differences in immune responses to SARS-CoV-2 that underlie disease outcomes. *Medrxiv*, 2020.06.06.20123414 (2020).
54. Z. Yang *et al.*, Absolute quantification of plasma cytokines and metabolome reveals the glycylproline regulating antibody-fading in convalescent COVID-19 patients. Metabolomics Workbench. https://www.metabolomicsworkbench.org/data/DRCCMetadata.php?Mode=Study&StudyID=ST001933. Deposited 21 October 2021.